Analysis and Simulation of a Single Generator-Infinite Bus Power System under Linear Quadratic Regulator Control

Ayokunle A. Awelewa, Ayoade F. Agbetuyi, Ishioma A. Odigwe, Isaac A. Samuel, Kenechukwu C. Mbanisi

Abstract— The thrust of this article is to develop elaborate educational material on linear quadratic regulator (LQR)-based power system control for electrical engineering students, especially senior undergraduate and fresh graduate students. The paper considers a comprehensive description of a power system, which is represented by a network of a single generator connected to an infinite bus, highlighting modeling, analysis, and simulation of the system. Graphical outputs for various combinations of system state and input weighting matrices are presented.

Index Terms— controllability and observability, linear quadratic regulator, model, single generator-infinite bus power system, state matrix, weighting matrix.

1 Introduction

Power system networks are interconnections of generating stations and loads by means of transmission lines that span several kilometers. The lines are high-tension cables that connect the generation to the transmission/sub-transmission substations and distribution cables that ultimately supply the customer loads. Moreover, a typical power system is a huge, complex network whose constitutive devices have different characteristics and response rates [1]. Therefore, its planning, design, operation, and maintenance require proper analysis and thorough understanding of various elements that compose it. It is, however, desirable that these elements operate together to ensure reliable, secure, and stable performance of the system at all time. Yet negative conditions or disturbances, such as single-phase to ground fault, three-phase to ground fault, sudden outage of large generation or load, etc., which may adversely affect the system do occur. Although the effect of these disturbances vary in degree depending on their location, type, and magnitude, their overall consequence is to shift the system from its steady-state operation, thereby making interconnected generators lose synchronism. So a significant power system operating criterion is that generating units remain in synchronism [1] during normal and abnormal conditions such that the system is kept stable and secure. Meanwhile, synchronous generator excitation control constitutes one of the most widely used methods to effect restoration of system stability—especially to dampen out local plant and inter-area mode oscillations—after the system has been perturbed [2], [3] and many excitation control schemes based on optimal control have been developed [4], [5], [6]. But the aim of this work is to use a simplified power system network to show the effect of varying system state and input weighting matrices on the dynamic performance of a power system. And this is particularly useful to beginners in the study of power system dynamics and control.

The rest of the paper is organized as follows. In section 2 a detailed description of the power system model employed is presented. In Section 3 a brief overview of linear quadratic regulator control is covered. Graphical outputs from system simulation as well as discussion of results are outlined in Section 4, and conclusions are drawn in Section 5.

2 System Model and Analysis

The power system network considered in this work is a single synchronous generator connected to an infinite bus. The generator and the infinite bus are interconnected through a number of transmission lines. A generic representation of this is shown in Fig. 1 [7], and a concise description, depicting a resultant impedance for all intermediate impedances between the generator and the infinite bus, is given by Fig. 2, where Rr and Xr are the resultant resistance and reactance, respectively.

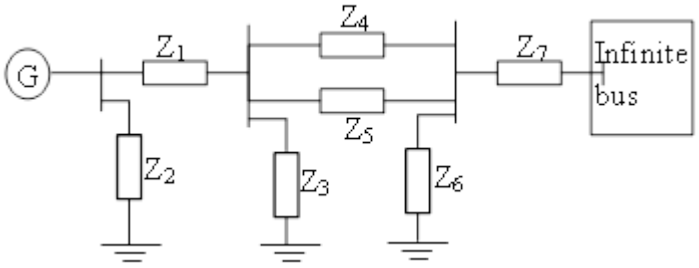

Fig. 1. Generic representation of an SMIB.

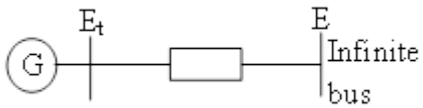

Fig. 2. Concise representation of an SMIB.

The considered network model, which comprises third-order state-space equations, is derived from the generator electro-mechanical performance equations as well as the equations representing the relationships between generator quantities, transmission line parameters, and infinite bus quantities. For

equations capturing the electrical characteristics of the generator, Fig. 3 [7] is apt. Here the dq0 transformation based on the two-reaction theory of synchronous machines [8] is employed. The transformation is a procedure for mapping the three phases of a synchronous generator into equivalent three axes—d-axis, q-axis, and zero-axis. (The zero-axis is a fictitious neutral axis included in order to have a valid invertible transformation.)

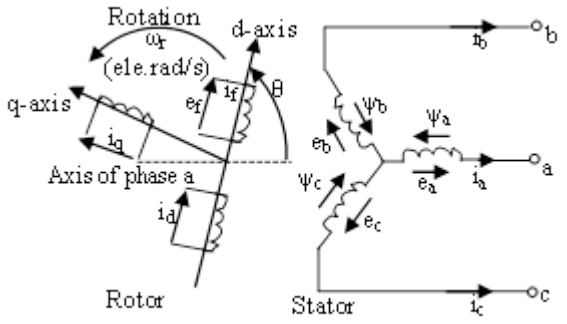

Fig. 3. Stator and rotor circuits of a synchronous generator.

In generating the electrical equations, one damper circuit each is located on the d-and q-axis, and the assumptions of sinusoidal distribution of stator windings along the air gap, negligibility of magnetic saturation and hysteresis effects, and constant rotor inductances *vis-a-vis* rotor position are considered [9], [10]. For stator circuits, the equations [7] are

$$v_d = p\psi_d - \psi_q\omega_r - R_a i_d \quad (1)$$

$$v_q = p\psi_q + \psi_d\omega_r - R_a i_q \quad (2)$$

$$v_0 = p\psi_0 - R_a i_0 \quad (3)$$

$$\psi_d = -(L_{ad} + L_l)i_d + L_{ad}i_{fd} + L_{ad}i_{1d} \quad (4)$$

$$\psi_q = -(L_{aq} + L_l)i_q + L_{aq}i_{1q} \quad (5)$$

$$\psi_0 = -L_0 i_0 \quad (6)$$

and for rotor circuits, the equations [7] are

$$v_{fd} = p\psi_{fd} + R_{fd}i_{fd} \quad (7)$$

$$0 = p\psi_{1d} + R_{1d}i_{1d} \quad (8)$$

$$0 = p\psi_{1q} + R_{1q}i_{1q} \quad (9)$$

$$\psi_{fd} = (L_{fd} + L_{ad})i_{fd} + L_{ad}i_{1d} - L_{ad}i_d \quad (10)$$

$$\psi_{1d} = L_{ad}i_{fd} + (L_{1d} + L_{ad})i_{1d} - L_{ad}i_d \quad (11)$$

$$\psi_{1q} = (L_{1q} + L_{aq})i_{1q} - L_{aq}i_q, \quad (12)$$

where

- v_d, v_q, v_0 : d-axis, q-axis, and neutral axis respective voltages
- v_{fd} : field voltage
- i_d, i_q, i_0 : d-axis, q-axis, and neutral axis respective currents
- i_{fd}, i_{1d}, i_{1q} : field and damper circuit currents
- R_a : armature resistance per phase
- R_{fd}, R_{1d}, R_{1q} : rotor circuit resistances
- ψ_d, ψ_q, ψ_0 : d-axis, q-axis, and neutral axis respective flux linkages
- $\psi_{fd}, \psi_{1d}, \psi_{1q}$: field and damper circuit flux linkages
- L_{ad} : d-axis mutual or magnetizing inductance
- L_{aq} : q-axis mutual or magnetizing inductance
- L_{fd}, L_{1d}, L_{1q} : rotor circuit leakage inductances
- L_l : stator circuit leakage inductance
- L_0 : neutral axis inductance
- p : differential operator (d/dt).

Equations (1)-(12), which are all given in per unit, form the fundamental expressions that completely depict the electrical characteristics of a synchronous generator. (The derivations are well spelt out in [7].)

To complete the mathematical equations of a synchronous generator, equations of motion (often called swing equation) showing its mechanical characteristics are given by [11], [12]

$$d\delta/dt = \omega \quad (13)$$

$$d^2\delta/dt^2 = 1/2H(P_m - P_e - D\,d\delta/dt), \quad (14)$$

where

δ = rotor angle (radians)
ω = rotor angular velocity (radians/s)
P_m = mechanical input power in per unit
P_e = electrical power in per unit
H = inertia constant in per unit
D = damping coefficient.

The electrical power in (14) is given in terms of the dq0 quantities as [7]

$$P_e = v_d i_d + v_d i_q + 2v_0 i_0. \quad (15)$$

And for a balanced system, (15) leads to

$$P_e = v_d i_d + v_d i_q. \quad (16)$$

For a lossless transmission line, i.e., $R_e = 0$ in Fig. 2, the equation relating the generator currents to the infinite bus bar voltage can be expressed as [9]

$$i_d = \frac{v_q - E\cos\delta}{x_e} \quad (17)$$

$$i_q = \frac{E\sin\delta - v_d}{x_e}, \quad (18)$$

where E is the infinite bus bar voltage.

Furthermore, neglecting the damper circuits, armature resistance, and the transformer voltage terms, $p\psi_d$ and $p\psi_q$, while assuming constant rotor speed [13], the combined voltage and flux linkage equations are

$$v_d = -\omega_0\psi_q \quad (19)$$

$$v_q = \omega_0\psi_d \quad (20)$$

$$v_{fd} = p\psi_{fd} + R_{fd}i_{fd} \quad (21)$$

and

$$\omega_0\psi_d = -(X_{ad} + X_l)i_d + X_{ad}i_{fd} \quad (22)$$

$$\omega_0\psi_q = -(X_{aq} + X_l)i_q \quad (23)$$

$$\omega_0\psi_{fd} = -X_{ad}i_d + (X_{ad} + X_{fd})i_{fd}, \quad (24)$$

respectively.

2.1 Nonlinear State-Space Model

Equations (13)-(24) are now used to develop the state-space equations. The swing equations, (13) and (14), constitute the first two state equations in which the rotor angle and the speed deviation are the state variables, i.e.,

$$\dot{\delta} = \omega \tag{25}$$

$$\dot{\omega} = 1/M\left(P_m - D\omega - P_e\right). \tag{26}$$

The equation describing P_e in terms of the network variables and parameters is derived in Appendix I (see (A.12)–(A.14)).

The third state variable is normally chosen to account for the field circuit dynamics, and therefore, the choice of field flux linkage, ψ_{fd}, is most appropriate. In some literature [14], [15], E'_q, which is the q-axis component of the voltage behind transient reactance X'_d, is chosen as the third state variable, but this choice is equivalent to that of the field flux linkage because the two variables are related by

$$E'_q = \frac{L_{ad}}{L_{ffd}}\psi_{fd} \tag{27}$$

The third equation is now given by (28). (See (A.1)–(A.11) in Appendix I.)

$$p\psi_f = u - \frac{(X_d + X_e)\psi_f}{\left(X'_d + X_e\right)T'_{do}} + \frac{\left(X_d - X'_d\right)E\cos\delta}{\left(X'_d + X_e\right)} \tag{28}$$

The complete non-linear state-space model [2], [16], [17] of the system is given by (29) below.

$$\begin{aligned}\dot{\delta} &= \omega\\ \dot{\omega} &= B_1 - A_1\omega - A_2\psi_f \sin\delta - \frac{B_2}{2}\sin 2\delta\\ \dot{\psi}_f &= u - C_1\psi_f + C_2\cos\delta\end{aligned} \tag{29}$$

where

$$A_1 = \frac{D}{M};\ A_2 = \frac{E}{M\left(X'_d + X_e\right)T'_{do}};$$

$$B_1 = \frac{P_m}{M};\ B_2 = \frac{E^2\left(X'_d - X_q\right)}{M\left(X'_d + X_e\right)\left(X_q + X_e\right)};$$

$$C_1 = \frac{\left(X_d + X_e\right)}{\left(X'_d + X_e\right)T'_{do}};\ C_2 = \frac{\left(X_d - X'_d\right)E}{\left(X'_d + X_e\right)}.$$

2.2 Linearized System State-Space Model

The aforementioned model can further be simplified by linearizing it about a known operating point. This is carried out by using the Taylor series expansion technique.

Therefore, expanding the non-linear state equation of eqn. 29 into a Taylor series about $\Omega_0 = [\delta_0\ \omega_0\ \psi_{f0}]$ and neglecting all the higher-order terms yields the matrix-form representation given by

$$\Delta\dot{\Omega} = A\Delta\Omega + B\Delta u \tag{30}$$

where

$$\Delta\Omega = \begin{bmatrix}\Delta\delta\\ \Delta\omega\\ \Delta\psi_f\end{bmatrix}$$

$$A = \begin{bmatrix}\frac{\partial f_1}{\partial\delta} & \frac{\partial f_1}{\partial\omega} & \frac{\partial f_1}{\partial\psi_f}\\ \frac{\partial f_2}{\partial\delta} & \frac{\partial f_2}{\partial\omega} & \frac{\partial f_2}{\partial\psi_f}\\ \frac{\partial f_3}{\partial\delta} & \frac{\partial f_3}{\partial\omega} & \frac{\partial f_3}{\partial\psi_f}\end{bmatrix}_{\Omega_0}$$

$$B = \begin{bmatrix}0\\ 0\\ \frac{\partial f_3}{\partial u}\end{bmatrix}_{u_0}$$

and

$$f_1(\Omega_0, u_0) = \dot{\delta}\big|_{\Omega_0, u_0}$$

$$f_2(\Omega_0, u_0) = \dot{\omega}\big|_{\Omega_0, u_0}$$

$$f_3(\Omega_0, u_0) = \dot{\psi}_f\big|_{\Omega_0, u_0}$$

$$\Delta\delta = \delta - \delta_0 \equiv \Delta\dot{\delta} = \dot{\delta} - f_1(\Omega_0, u_0)$$

$$\Delta\omega = \omega - \omega_0 \equiv \Delta\dot{\omega} = \omega - f_2(\Omega_0, u_0)$$

$$\Delta\psi_f = \psi_f - \psi_{f0} \equiv \Delta\dot{\psi}_f = \dot{\psi}_f - f_3(\Omega_0, u_0)$$

$$\Delta u = u - u_0.$$

2.3 System Stability and State Matrix Analysis

The parameters of the system considered in this work are [2]:

$X_d = 1.25$ $X'_d = 0.3$ $X_q = 0.7$ $T'_{do} = 9.0$

$M = 0.0185$ $D = 0.005$ $X_e = 0.2$ $E = 1.0$

The initial values of u and Pm are assumed to be 1.1p.u. and 0.725p.u. respectively, while the steady-state values of the system variables are given as [2]:

$\delta_i = 0.7438$ $\omega_i = 0$ $\psi_{fi} = 7.7438$

From the above-given information, the values of A_1, A_2, B_1, B_2, C_1, C_2, are computed as A_1=0.270, A_2= 12.012, B_1 = 39.189, B_2 = -48.048, C_1 = 0.323, and C_2 = 1.9, and are used to evaluate all the elements of the Jacobian (state) matrix, A, and those of the input vector, B, in the linearized system model as follows:

$$\left.\frac{\partial f_1}{\partial\delta}\right|_{\Omega_0, u_0} = 0;\ \left.\frac{\partial f_1}{\partial\omega}\right|_{\Omega_0, u_0} = 1;\ \left.\frac{\partial f_1}{\partial\psi_f}\right|_{\Omega_0, u_0} = 0$$

$$\left.\frac{\partial f2}{\partial \delta}\right|_{\Omega_0,u_0} = 48.048\cos 2\delta 0 - 12.012\psi f 0\cos\delta 0 = -64.534;$$

$$\left.\frac{\partial f2}{\partial \omega}\right|_{\Omega_0,u_0} = -0.270;$$

$$\left.\frac{\partial f2}{\partial \psi f}\right|_{\Omega_0,u_0} = -12.012\sin\delta 0 = -8.1533;$$

$$\left.\frac{\partial f3}{\partial \delta}\right|_{\Omega_0,u_0} = -1.9\sin\delta 0 = -1.2896; \left.\frac{\partial f3}{\partial \omega}\right|_{\Omega_0,u_0} = 0;$$

$$\left.\frac{\partial f3}{\partial \psi f}\right|_{\Omega_0,u_0} = -0.323; \left.\frac{\partial f3}{\partial u}\right|_{\Omega_0 u_0} = 1.$$

And substituting these values into (30) leads to (31) below.

$$\begin{pmatrix}\Delta\dot{\delta}\\ \Delta\dot{\omega}\\ \Delta\dot{\psi}f\end{pmatrix} = \begin{pmatrix}0 & 1 & 0\\ -64.534 & -0.270 & -8.1533\\ -1.2896 & 0 & -0.323\end{pmatrix}\begin{pmatrix}\Delta\delta\\ \Delta\omega\\ \Delta\psi f\end{pmatrix} + \begin{pmatrix}0\\ 0\\ 1\end{pmatrix}\Delta u \tag{31}$$

The stability of the linearized system can now be determined using the Lyapunov's indirect stability method (otherwise known as the second method of Lyapunov). It states that if a non-linear system is linearized about its operating point, and it's observed that the resulting linearized model is strictly stable (i.e., all the eigenvalues of its state matrix are strictly in the left-half complex plane), then the equilibrium point for the actual non-linear system is asymptotically stable [15]. Computing the eigenvalues, λ_1, λ_2, λ_3, of the system using the MATLAB function *eig*, we have λ_1 = -0.2165 + 8.0315i, λ_2 = -0.2165 – 8.0315i, and λ_3 = -0.16, so the stability condition is met. Likewise, the state controllability and observability of the system can be determined by performing the Kalman test [18]. It states that a dynamical system is completely state controllable if and only the rank of an *n* x *n* controllability matrix

$$\begin{bmatrix}\mathbf{B} & \mathbf{AB} & \mathbf{A}^2\mathbf{B} & \cdots & \mathbf{A}^{n-1}\mathbf{B}\end{bmatrix} \tag{32}$$

is *n*; also, the system is completely state observable if and only if the rank of an *n* x *nm* observability matrix

$$\begin{bmatrix}\mathbf{C}\\ \mathbf{CA}\\ \mathbf{CA}^2\\ \vdots\\ \mathbf{CA}^{n-1}\end{bmatrix} \tag{33}$$

is *n*. (Here *n* represents the order of the system and *m* the number of system outputs.)

Therefore, using (32) and (33), we can find the controllability and observability matrices (indicated by *M* and *N*, respectively) of the system given in (31) as

$$M = \begin{pmatrix}0 & 0 & -8.1533\\ 0 & -8.1533 & 4.8349\\ 1 & -0.3230 & 8.1043\end{pmatrix}; N = \begin{pmatrix}1 & 0 & -64.5340\\ 0 & 1 & -0.2700\\ 0 & 0 & -8.1533\end{pmatrix}.$$

3 LQR DESIGN

The linear quadratic regulator establishes an optimal control law for a linear system with a quadratic performance index. Given the linearized system model in (31), the problem here is to determine the matrix **K** of the optimal control law

$$\Delta\mathbf{u} = -\mathbf{K}\Delta\mathbf{\Omega} \tag{34}$$

in order to minimize the performance index

$$J = \int_0^\infty \left(\Delta\mathbf{\Omega}^T\mathbf{Q}\Delta\mathbf{\Omega} + \Delta\mathbf{u}^T\mathbf{R}\Delta\mathbf{u}\right)dt, \tag{35}$$

where **Q** is a positive-definite (or positive-semidefinite) Hermitian or real symmetric matrix, **R** is a positive-definite Hermitian or real symmetric matrix, and $\Delta\mathbf{\Omega}$ is the state vector. Substituting (34) into (35) yields

$$J = \int_0^\infty \Delta\mathbf{\Omega}^T\left(\mathbf{Q} + \mathbf{K}^T\mathbf{R}\mathbf{K}\right)\Delta\mathbf{\Omega}dt \tag{36}$$

Thus minimizing J in (36) results in the gain matrix [18], [19]

$$\mathbf{K} = \mathbf{R}^{-1}\mathbf{B}^T\mathbf{P}, \tag{37}$$

where **P** is a positive-definite Hermitian or real symmetric matrix that satisfies the reduced Riccati equation

$$\mathbf{A}^T\mathbf{P} + \mathbf{P}\mathbf{A} - \mathbf{P}\mathbf{B}\mathbf{R}^{-1}\mathbf{B}^T\mathbf{P} + \mathbf{Q} = \mathbf{0}, \tag{38}$$

4 SYSTEM SIMULATION

The system is now simulated in MATLAB to show its performance for various sets of values of Q and R. First, the open-loop behavior of the system is shown in Fig. 4. Then for the closed-loop (LQR-controlled) system performance, two cases of the weighting matrices Q and R are considered. In the first case, R is fixed and Q is varied, while in the second case R is varied and Q is fixed.

So the responses in Figures 5-8 show the case when **R** = 1 and **Q** = 0.1***I**, **I**, 5***I**, and 15***I**, and likewise, those in Figures 9-11 show the case when **Q** = 15***I** and **R** = 0.1, 0.2, and 0.8. (Here **I** is 3 x 3 identity matrix.)

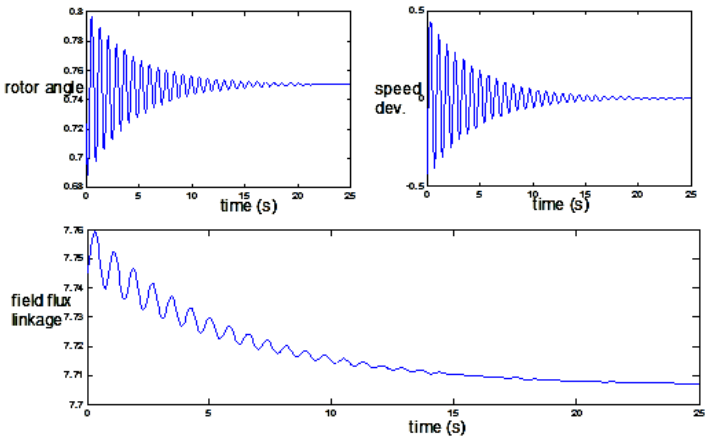

Fig. 4. System open-loop characteristics.

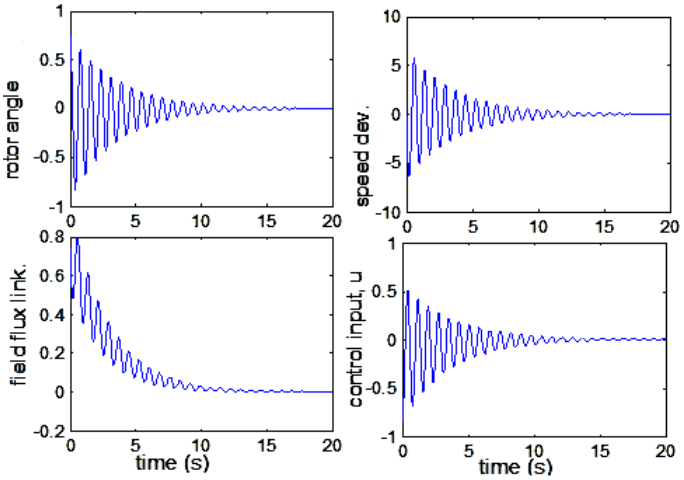

Fig. 5. LQR-controlled system characteritics (when Q = 0.1*$\mathbf{I}$; R = 1).

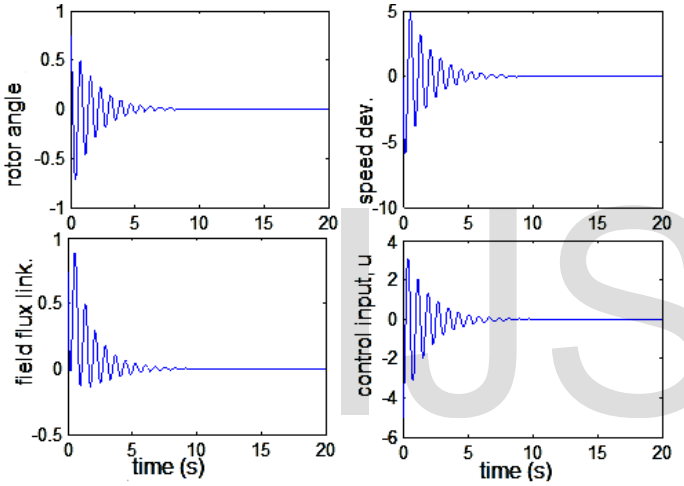

Fig. 6. LQR-controlled system characteritics (when Q = $\mathbf{I}$; R = 1).

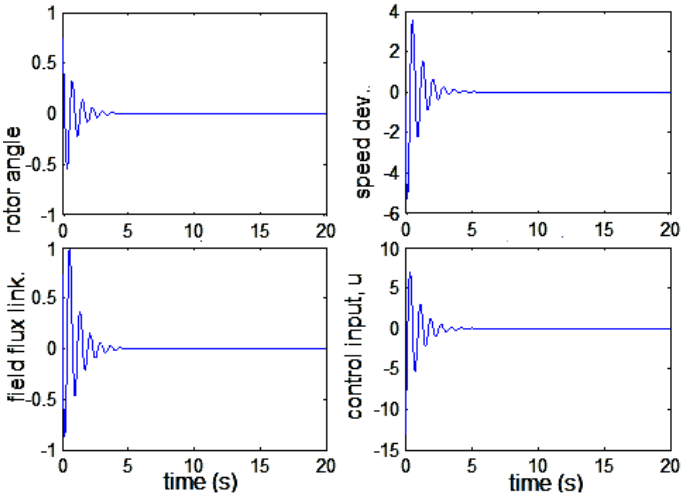

Fig. 7. LQR-controlled system characteritics (when Q = 5*$\mathbf{I}$; R = 1).

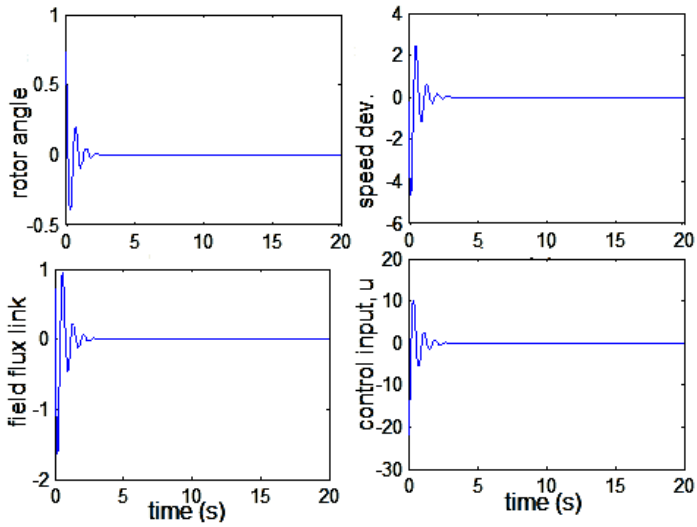

Fig. 8. LQR-controlled system characteritics (when Q = 15*$\mathbf{I}$; R = 1).

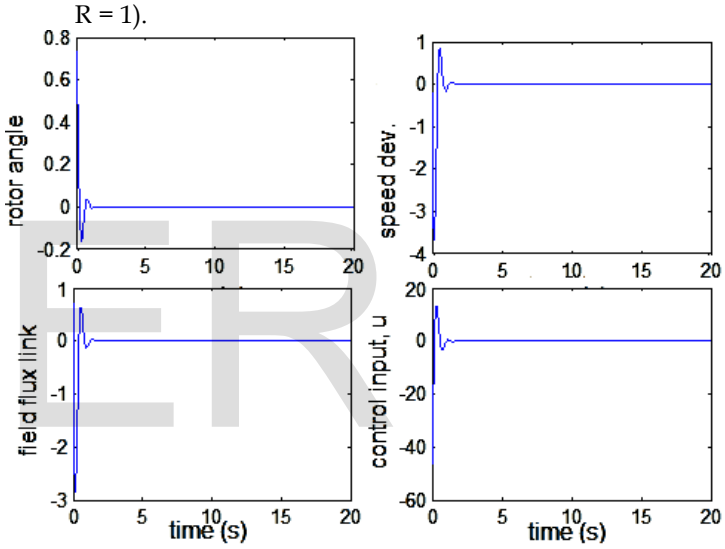

Fig. 9. LQR-controlled system characteritics (when Q = 15*$\mathbf{I}$; R = 0.1).

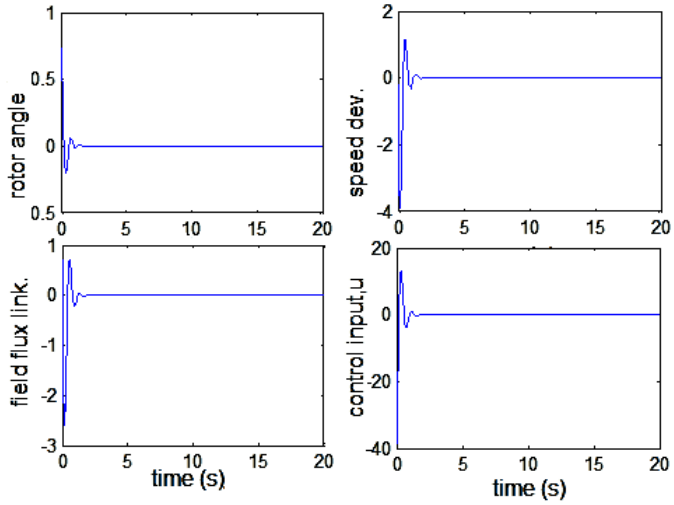

Fig. 10. LQR-controlled system characteritics (when Q = 15*$\mathbf{I}$; R = 0.2).

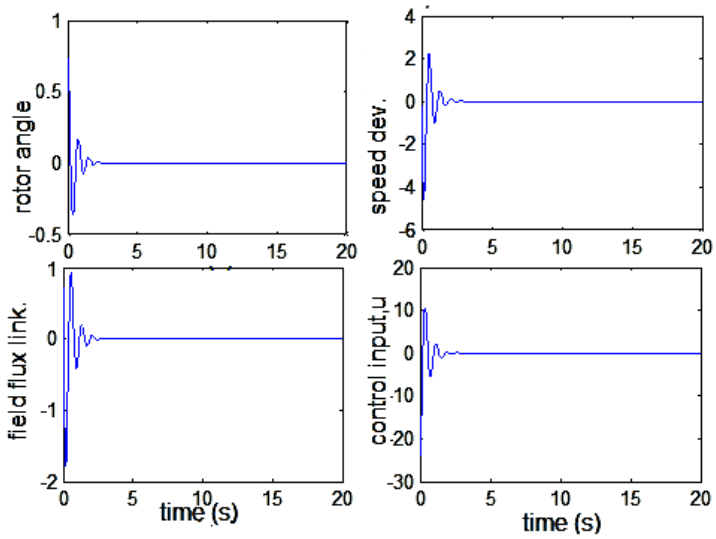

Fig. 11. LQR-controlled system characteritics (when Q = 15*I; R = 0.8).

From the analysis of the system characteristics, it could be inferred that though the system is stable, controllable and observable, oscillations of the system variables (rotor angle, for instance) take unbearably and undesirably long time (more than 25s) to dampen out. Also, it could be inferred that the performance of the system, when controlled by the LQR, varies depending on the combination of the state and control weighting matrices, **Q** and **R**. When **R** is fixed and **Q** is gradually increased, the system dynamic performance shows significant improvement with a price of increased control effort though. Specifically, better performance is recorded when **Q** = 15**I** and **R** =1 than at any other value of **Q** with the same **R**. It is also observed that with this value of **Q** and varying values of **R**, the behavior of the system improves greatly appreciably. Notably, at **Q** = 15I and **R**= 0.1, best dynamic performance is realized without much control activity—the maximum overshoot and the settling time for rotor angle are 0.033 and 1.5s, respectively.

5 CONCLUSION

A description, analysis, and LQR-based control of a single generator connected to an infinite bus have been considered in this paper. Specifically, stability, controllability, and observability of the system have been established using a linearized version of the nonlinear model describing the system. Also, investigation of the system dynamic performance has been carried out under linear quadratic regulator control for various combinations of input and state weighting matrices, with well displayed graphical outputs to show the results of the system simulation.

APPENDIX

Choosing ψ_{fd} as the third state variable, we can derive (28) in the body of the paper as follows:
Combining (21) and (24) and solving for i_{fd} result in

$$i_{fd} = \frac{v_{fd} + L_{ad} i_d p}{(L_{ad} + L_{fd})p + R_{fd}}. \quad \text{(A1)}$$

Substituting (A1) into (22) gives

$$\omega_0 \psi_d = -(X_{ad} + X_l) i_d + X_{ad}\left(\frac{v_{fd} + L_{ad} i_d p}{(L_{ad} + L_{fd})p + R_{fd}}\right)$$

$$= \frac{X_{ad} v_{fd}}{(L_{ad} + L_{fd})p + R_{fd}} - \left((X_{ad} + X_l) - \frac{X_{ad} L_{ad} p}{(L_{ad} + L_{fd})p + R_{fd}}\right) i_d$$

$$= \frac{v_{fd}}{1 + T'_{do} p}\frac{X_{ad}}{R_{fd}} - \left(\frac{X_{ad}\frac{L_{fd} p}{R_{fd}} + \left(\frac{L_{ad} p + L_{fd} p}{R_{fd}} X_l\right) + X_{ad} + X_l}{1 + T'_{do} p}\right) i_d$$

$$= \frac{v_{fd}}{1 + T'_{do} p}\frac{X_{ad}}{R_{fd}} - \left(\frac{\frac{1}{R_{fd}}\left(\frac{L_{ad} L_f}{L_{ad} + L_l} + \frac{(L_{ad} + L_{fd}) L_l}{L_{ad} + L_l}\right) p + 1}{1 + T'_{do} p}\right) X_d i_d$$

$$= \frac{u + p T'_{do}\left(X_d - X'_d\right) i_d}{1 + T'_{do} p} - X_d i_d \equiv X_{ad} i_{fd} - X_d i_d \quad \text{(A2)}$$

Variable u in (A2) is defined as

$$u = \frac{v_{fd} X_{ad}}{R_{fd}}.$$

Let Em (where Em is an arbitrary variable) be given as

$$E_m = X_{ad} i_{fd} = \frac{u + p T'_{do}\left(X_d - X'_{do}\right) i_d}{1 + T'_{do} p} \quad \text{(A3)}$$

Also, from (21), a new term $p\psi_f$ is obtained in terms of $p\psi_{fd}$ as illustrated below.

$$p\psi_{fd} = v_{fd} - R_{fd} i_{fd} = \frac{R_{fd}}{X_{ad}}(u - X_{ad} i_{fd})$$

Hence,

$$p\psi_f = u - X_{ad} i_{fd} = u - E_m, \quad \text{(A4)}$$

where

$$\psi_f = \frac{X_{ad}}{R_{fd}}\psi_{fd}.$$

And by combining (A3) and (A4), ψ_f can be expressed as

$$\psi_f = T'_{do}\left(E_m - \left(X_d - X'_d\right) i_d\right) \quad \text{(A5)}$$

Again, from (19), (20), (23), and (A2), vd and vq can be obtained as

$$v_d = X_q i_q \quad \text{(A6)}$$

$$v_q = E_m - X_d i_d \quad \text{(A7)}$$

By using (A6) and (A7), (17) and (18) can be rewritten as

$$i_d = \frac{E_m - E\cos\delta}{X_d + X_e} \quad \text{(A8)}$$

$$i_q = \frac{E\sin\delta}{X_q + X_e} \quad \text{(A9)}$$

Em can now be obtained in terms of ψ_f by using (A5) and (A8).

$$Em = \frac{(Xd + Xe)\psi f}{\left(X'd + Xe\right)T'do} \frac{\left(Xd - X'd\right)E\cos\delta}{\left(X'd + Xe\right)} \quad (A10)$$

By using (A10), (A4) can be rewritten as

$$p\psi f = u - \frac{(Xd + Xe)\psi f}{\left(X'd + Xe\right)T'do} + \frac{\left(Xd - X'd\right)E\cos\delta}{\left(X'd + Xe\right)} \quad (A11)$$

Equation (A11) is now the third state equation (see (28)).
Also, an expression for Pe is computed by using (16) and (A6) – (A10) as follows

$$Pe = vdid + vqiq = Xqiqid + Emiq - Xdidiq \quad (A12)$$

Also,

$$Pe = \frac{(Xq - Xd)E\sin\delta}{(Xq + Xe)(Xd + Xe)}Em + \frac{E\sin\delta}{Xq + Xe}Em - \frac{(Xq - Xd)E^2\sin2\delta}{2(Xq + Xe)(Xd + Xe)},$$

which, after simplification, gives

$$Pe = \frac{E\psi f \sin\delta}{\left(X'd + Xe\right)T'do} + \frac{\left(X'd - Xq\right)E^2\sin2\delta}{2(X'd + Xe)(Xq + Xe)} \quad (A13)$$

REFERENCES

[1] CIGRE Joint Task Force on Stability Terms and Definitions, "Definition and Classification of Power System Stability," IEEE Trans. Power Systems, vol. 19, no. 2, pp. 1387-1401, May 2004.

[2] L.N. Wedman and Y.N. Yu, ''Computation techniques for the stabilization and optimization of high order power systems,'' IEEE Power Industry Computer Applications Conference Record, pp. 324-343, 1969.

[3] P. Kundur, D.C. Lee and H.M. Zein El-Din, ''Power system stabilizers for thermal units: Analytical Techniques and on-site validation,'' IEEE Transactions, Vol. PAS-100, pp. 81-95, January 1981.

[4] Q. Lu and Z. Xu, ''Decentralized non-linear optimal excitation control,'' IEEE Transactions on Power Systems, vol. 11, no. 4, pp. 1957-1962, November 1996.

[5] S. Takada, ''Compensation of bus voltage fluctuation by means of optimal control of synchronous machine excitation,'' Elec. Eng. Jap. (USA), vol. 8, pp. 42-52, 1968.

[6] A. Ghandakly, P. Kronegger, "An Adaptive Time-Optimal Controller for Generating Units Stabilizer Loops," IEEE-PES Trans. Power Systems, vol. PWRS-2, no. 4, pp. 1085-1090, November 1987.

[7] P. Kundur, ''Power system analysis and control,'' McGraw-Hill Book Company, New York, 1994.

[8] G. Krong, ''Two–reaction theory of synchronous machines-part 2,'' AIEE Transactions, vol. 52, pp. 352-355, June 1933.

[9] B.K. Mukhopadhyay and M.F. Malik, "Optimal control of synchronous machine excitation by quasilinearisation techniques," IEEE Proceedings, vol. 119, no. 1, pp. 91-98, 1972.

[10] M.F. Hasan and M.G. Singh, ''A hierarchical model-following controller for certain non-linear systems,'' Int. J. Systems Sc., vol. 7, no. 7, pp. 727-730, 1976.

[11] H. Saadat, "Power System Analysis," McGraw-Hill Book Company, Tata, 2002.

[12] P.M. Anderson and A.A. Fouad, "Power System Control and Stability," The IEEE Press, Power Engineering Society, Piscataway, NJ, 2003.

[13] M.S. Ghazizadeh and F.M. Hughes, "A generator transfer function regulator for improved excitation control," IEEE Transactions on Power Systems, vol. 13, no. 2, pp. 435-441, May 1998.

[14] D. Gan, Z. Qu and H. Cai, "Multi-machine power system excitation control design via theories of feedback linearization control and robust control," International Journal of Systems Science, vol. 31, no. 4, pp. 519-527, 2000.

[15] Jean Jaques E. Slotine, and Weiping Li, ''Applied Non-linear Control,'' Prentice-Hall Edition, New Jersey, 1991.

[16] P.C. Park, "Lyapunov redesign of model reference adaptive control systems," IEEE Transactions, Automatic Control, AC-11, pp. 362-365, 1989.

[17] M. Nambu and Ohsawa Y., "Development of an advanced power system stabilizer using a strict linearization approach," IEEE Transactions on Power Systems, vol. 11, pp. 813-818, 1996.

[18] K. Ogata, "Modern Control Engineering," Third Edition, Prentice Hall, Upper Saddle River, New Jersey, 1997.

[19] R.S. Burns, ''Advanced Control Engineering,'' Butterworth-Heinemann Edition, Woburn, 2001.

Ayokunle A. AWELEWA is with the Department of Electrical & Information Engineering, Covenant University, Canaan Land, Ota, Nigeria. His research areas include power system stabilization and control, and modeling and simulation of dynamical systems.

Ayoade A. Agbetuyi is with the Department of Electrical & Information Engineering, Covenant University, Canaan Land, Ota, Nigeria. His research areas include renewable energy, power system stability and reliability, and distributed generation and renewable energy.

Ishioma A. Odigwe is with the Department of Electrical & Information Engineering, Covenant University, Canaan Land, Ota, Nigeria. His research areas include distribted generation with renewable energy sources, and power system stability analysis.

Isaac A. SAMUEL is with the Department of Electrical & Information Engineering, Covenant University, Canaan Land, Ota, Nigeria. His research areas include power system operation, reliability, and maintenance.

Kenechukwu C. Mbanisi is a former student (September 2008- July 2013) of the Department of Electrical & Information Engineering, Covenant University, Ota, Nigeria. He is profoundly interested in and enthusiastic about modeling, analysis, and control of dynamical systems.